On the Colors of Faint Galaxies

Roland Buser

Abstract

The role of color determinations in the context of galaxy evolution and cosmology is briefly described. A rough sketch is given of spectral evolutionary models of galaxies and their use in computing synthetic galaxy colors and magnitudes as functions of redshift. Bruzual and Kron's (1980) application of these theoretical calculations in the analysis of the observations of a complete sample of faint galaxies is discussed as an important and promising step toward the solution of the perennial riddle of the universe and its galaxies, via multicolor photometry.

Cosmology and Galaxy Evolution

Naturally, the most prominent index of a star's evolution is its luminosity changing with time. If a galaxy is a 'closed' system of stars and gas that was or still is transforming gas into stars, we must expect the galaxy's luminosity to change with time accordingly. As for the stars themselves, the time scale for galactic evolution is so large as to prevent us from observing the evolution of any one galaxy directly. Yet we can hope that the simultaneous observation of many galaxies reveals us different stages in the lives of galaxies, from which we might be able to recover a natural sequence of stages in the evolutionary history of the typical galaxy. – How, then, would we wish to tackle the problem of galaxy evolution?

Consider, first, the real home of the galaxies: the universe. The universe is so large that by looking at its galaxies in its ever deeper realms we effectively see these galaxies at ever more distant past times. Since galaxy luminosities are likely to be limited by general astrophysical constraints, galaxies at larger distances have, on the average, fainter apparent magnitudes; the relation is not a strict one because, for a given apparent magnitude, for each galaxy there is of course a luminosity-distance ambiguity. Still, it can be said that comparing galaxies at successively larger distances holds a clue to the evolution of galaxies, and this necessarily involves observations at faint magnitude levels.

Consider now the real context of galaxy evolution: the evolution of the universe itself. The most fundamental observable dimension of the evolving universe is not the distance, but the redshift. There is no ambiguity in the redshift-distance relation for galaxies. Hence galaxies at successively larger redshifts are also at successively larger distances and thus sample increasingly past cosmic epochs. The study of faint galaxies at different redshifts is therefore a promising approach to the evolution of galaxies.

Consider, finally, the number of galaxies as a function of apparent magnitude and redshift, $A(m,z)$. If we assume space to be homogeneously and isotropically populated with galaxies, then the number of galaxies, $A(z)$, in a redshift shell of radius z and thickness dz is proportional to the volume of this redshift shell, i.e., $A(z)$ samples the (differential) volume element dV/dz, which is predicted different for different values of the deceleration parameter, q_0, in Friedmann models of the universe. Hence $A(z)$ is a cosmological test, providing q_0. Knowledge of this value of q_0 then allows us to determine the (luminosity) evolution as a function of redshift by studying the Hubble diagram (i.e., the (m,z) relation) and the count-magnitude diagram (i.e., the $A(m)$ relation) of the sample galaxies. Adoption of a value for H_0, the Hubble expansion parameter, eventually gives the evolution as a function of time via the time-redshift relation, which depends on q_0 and scales as H_0^{-1} (Sandage 1961).

141

This line of thought, then, suggests that in order to get hold of the evolution of galaxies, magnitudes and redshifts be obtained for large numbers of faint galaxies. – But how can redshifts be determined for large numbers of faint galaxies? That's the time for the colors to enter the scene.

Color and Redshift

The color of a galaxy is obtained from observations of its integrated brightnesses in two or more fixed wavelength bands typically several hundred Angstroms wide. Such a color is a coarse measure of spectral information and is therefore apt to reflect the redshift of its underlying spectral energy distribution in principle. In practice we can compute, by artificially redshifting the known intrinsic spectral energy distribution of a galaxy, the fluxes falling into the fixed photometric bands at successive redshift steps and produce colors as a function of redshift for that particular galaxy. Indeed, galaxy colors as a function of redshift represent the very kind of structure that we are looking for in order to determine redshifts from observed colors.

In the present context, the practical application requires that at least two rather important complications to the above simple procedure be taken into account.

First, different galaxies at zero redshift span a range of colors to begin with, due to their different intrinsic spectral energy distributions. The distribution of colors of bright galaxies may lead us to think of the morphological type of galaxy as the fundamental variable behind the observed variations in the spectral energy distributions. Relations between color and redshift must therefore be evaluated for different morphological galaxy types.

Second, any relations between color and redshift computed by artificially redshifting available bright galaxy spectra (observed at $z \approx 0$) necessarily ignore the time-redshift relation. In order to interpret the observed colors of truly reshifted galaxies, color evolution as a function of redshift (hence time) needs to be taken into account.

For lack of observed spectral energy distributions of galaxies of different morphologi-

cal types and redshifts, these requirements imply that evolving spectra of galaxies be modeled.

Spectral Evolution of Galaxies

Modeling the spectral evolution of galaxies assumes that a galaxy is a closed system of gas and stars. At any given time the emitted spectral energy distribution of the galaxy is the sum of the absolute spectral energy distributions of all the stars existing in the galaxy at that time. The number of stars that contribute to the galaxy's luminosity at a given time is the difference between the number of stars that have been born out of the galaxy's gas, and the number of stars that have finished their active lives by that time. Both numbers of stars in this difference are functions of time: the first is given by the star formation rate, and the second results from applying stellar evolution theory to the stars formed. Since the time scale for stellar evolution is a function of the stellar mass, it is assumed that via the star formation rate gas is transformed into stars according to a stellar mass spectrum (i.e., the initial mass function), which itself is assumed to be independent of time and to be of the same general form as the stellar mass function observed in the solar neighborhood (Salpeter 1955).

For each stellar mass and for any given time, a theoretical evolutionary track provides the observable quantities like spectral type or B-V color, and absolute magnitude, which in turn determine the selection of the associated stellar spectral energy distribution from a comprehensive library of spectrophotometric data. Adding all the stellar spectra corresponding to the stars in the galaxy at a given time yields, finally, the spectral energy distri-

Fig. 1. Examples of evolving energy distributions for galaxy models with different assumed histories of the star formation rate (see text). The distributions are shown at different ages from 1 to 16 Gyr, as indicated. For comparison, the observed spectral energy distribution of a typical nearby elliptical galaxy (obs.) is displayed on the same flux scale, but with an arbitrary shift of the zero point. Note the pronounced differences between the models in the evolution of their ultraviolet spectra ($\lambda \lesssim 4000$ Å), which will show up as color differences in the visual wavelength range if such galaxies are observed at high redshift ($z \approx 1$). (Figure adapted from Bruzual 1981.)

i Model

obs.

c = 0.7 Model

obs.

143
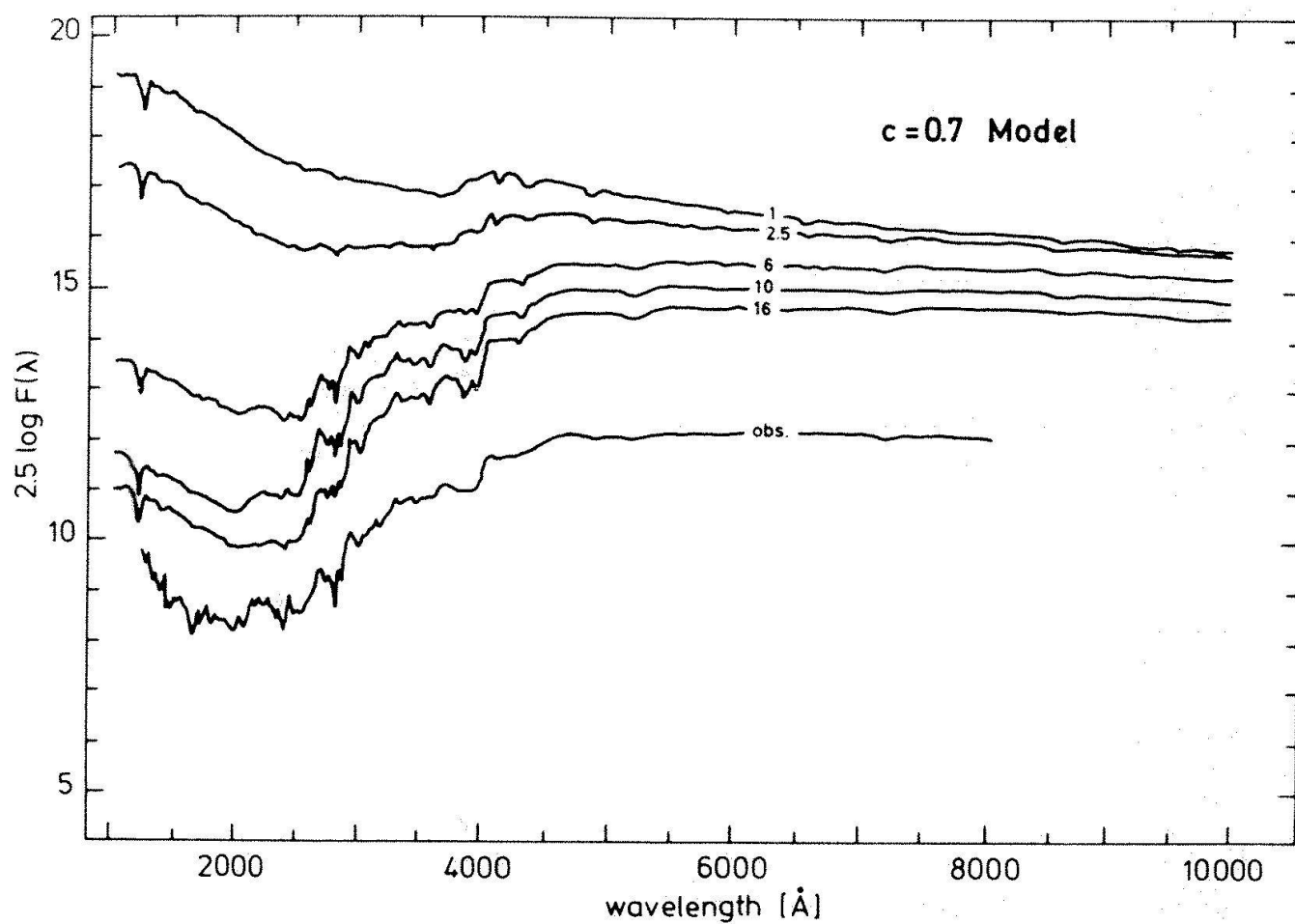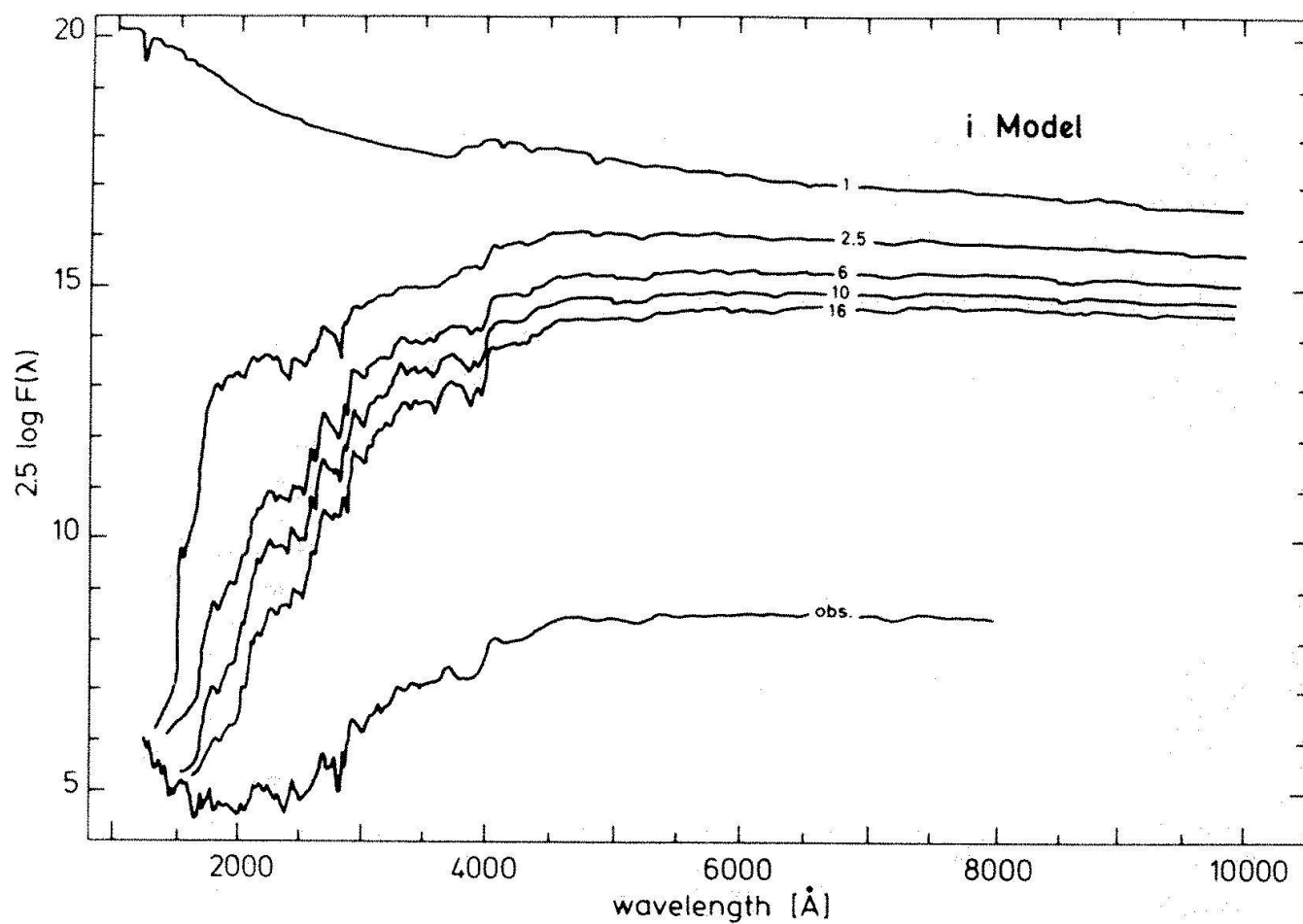
bution of the whole galaxy, at that particular time.

A galaxy spectral evolutionary model then consists of a series of absolute spectral energy distributions calculated, according to the above scheme, for different times.

The most important parameter of such a model is the star formation rate as a function of time. For example, observations of elliptical galaxies suggest that these systems contain mainly old stars and little gas. Hence star formation was probably very efficient and exhaustive at early stages of their evolution. On the other hand, observations of spiral and irregular galaxies reveal considerable amounts of gas and significant star formation still going on at their present – i.e., presumably late – evolutionary phases. Dwarf galaxies, still, appear to have started their lives as rather low-density systems, with a low star formation rate that may reach its highest value only at late times in their evolution.

Most currently available models (e.g., Tinsley 1980, Bruzual 1981) attempt to approximate analytically these different histories of star formation in galaxies, as suggested by the observed properties of different morphological types. 'Initial burst (i) models' have a high constant star formation rate during the first billion years or so, after which star formation ceases. For 'continuous burst (c) models' the star formation rate is highest at the beginning and thereafter decreases exponentially, the time scale for the decrease being a free parameter, which allows the gas mass to total mass ratio at the present time to cover the observed range. 'Delayed burst (d) models' start with a low but growing star formation rate which peaks after an adjustable time scale (e.g., 10 Gyr).

Figure 1 illustrates a few important aspects of such theoretical models constructed by Bruzual (1981). Evolving galaxy spectra at ages between 1 and 16 Gyr are shown for an i-model (upper panel) and for a c-model (lower panel). While there is a similarly slow change with time of the slope of the visual and near-infrared spectra of both models, the evolutionary differences between the models are most prominent in the ultraviolet. The absence of star formation after 1 Gyr makes the i-model get rapidly darker at ultraviolet wavelengths and its whole spec-

trum dominated by late-type giant stars; on the other hand residual formation of massive hot stars throughout the life of the c-model provides the main source of its less rapidly dimming ultraviolet light.

The curves labeled 'obs.' represent the observed spectrum of a typical nearby elliptical galaxy and are displayed to illustrate how the models can be checked on their ability to match real galaxies. In view of the scarcity of presently available observations of ultraviolet galaxy spectra – which are most important in putting constraints on the adopted histories of star formation –, the main purpose of such comparisons is to ascertain that the variety of observed galaxy spectra be covered by a variety of evolving model energy distributions at the same present age.

The variety of model energy distributions as functions of time can then be used to calculate the colors and magnitudes of the model galaxies as functions of redshift, after a cosmological model has been specified (i.e., values for q_0 and H_0 have been adopted), providing the time-redshift relation and an age of the universe consistent with the adopted epoch for galaxy formation.

Figures 2a and 2b give examples of the resulting relations for the J-F color and the F magnitude defined by Kron's (1980a) photographic broad-band system. The curves in both figures are for the same representative models of galaxies having present ages of 16 Gyr, adopted in a Friedmann universe with $H_0 = 50$ km s^{-1} Mpc^{-1} and $q_0 = 0$. The top curves are for a nonevolving galaxy, i.e., with an i-model spectrum frozen at its present age. The other curves are for evolving galaxy models, labeled according to their particular values for the star formation rate parameter, a lower numerical value for the c-models meaning that gas consumption – or star formation – decreases more slowly with time.

Qualitatively, these results demonstrate quite generally – although Figures 2 are for a particular color system – that evolution has a significant effect on the colors and magnitudes of galaxies, making them bluer and brighter, at all redshifts, than an hypothetically unevolving source of the same present color and absolute magnitude. Galaxies which by the present time have the same intrinsic colors and absolute magnitudes may
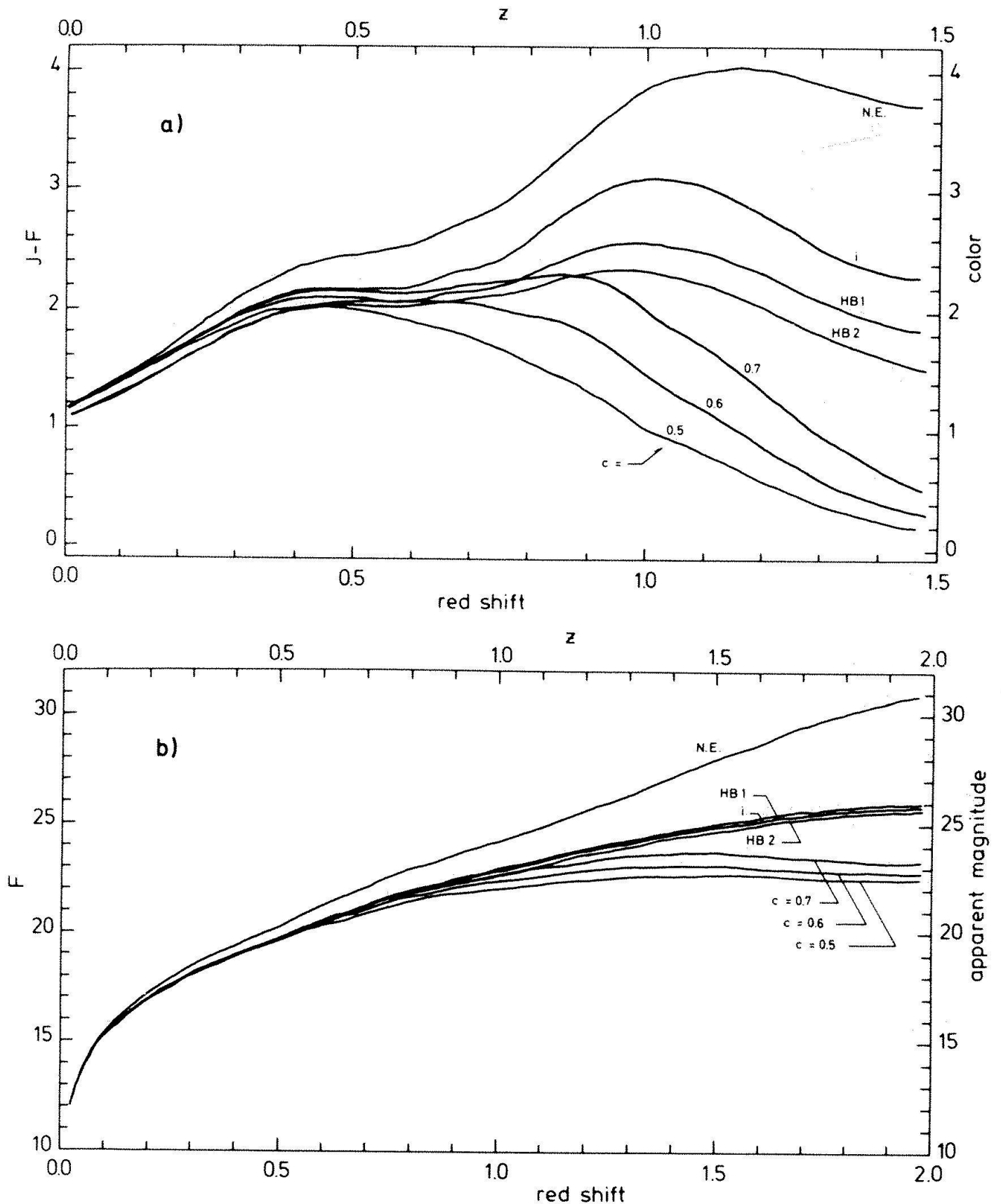
144

Fig. 2. Curves of intrinsic J-F color (a) and apparent F magnitude (b) as functions of redshift, for representative galaxy models. The curves labeled N.E. were computed from the i-model spectrum at the present age (z = 0), i.e., from an unevolving source. The differences between the N.E. and the i-model curves therefore illustrate the evolutionary effects, which operate in addition to the k-correction. Curves labeled HB1 and HB2 refer to the i-model with horizontal branch star light added. For the c-models, a lower numerical value indicates that the star formation rate decreases more slowly with time. In Figure 2b, all models were normalized to the same absolute magnitude at their present age.

(Figures adapted from Bruzual 1981.)

in fact have evolved into this specific condition on rather different routes and through widely dispersed colors and luminosities at earlier epochs.

Quantitatively, such predictions for galaxy colors and magnitudes as functions of redshift can now be exploited in the interpretation of the observed colors and magnitudes of faint galaxies.

Counts and Colors of Faint Galaxies

As we have seen in the previous sections, cosmology and galaxy evolution are two strongly connected subjects. The present approach to these subjects pursues the questions: How many galaxies are there in the universe in redshift shells of successively larger radius, and what is the distribution of the apparent galaxy brightnesses in each of these shells? Technically, this problem translates into the quest for the number of galaxies as a function of apparent magnitude and redshift, $A(m, z)$. Since this necessarily involves large numbers of faint galaxies, a more practicable step toward $A(m, z)$ consists in studying the number of galaxies as a function of apparent magnitude and color, $A(m, c)$, where the color c serves as a substitute for the redshift, due to the existence of a color-redshift relation, $c(z)$ (Figure 2a). Because different morphological galaxy types trace out different $c(z)$ relations, and because each of these may be multiple-valued (i.e., a given value of c may correspond to different values of z), several colors rather than a single one will eventually be needed to determine $A(m, z)$ from observations.

The interpretation of faint galaxy data rests on our knowledge of the corresponding data for bright galaxies. More to the point: from the local properties of the universe, as reflected by the number density, the luminosity function, and the intrinsic color distribution of galaxies observed at bright magnitudes (i.e., $z \approx 0$), the numbers and the distributions of apparent magnitudes and intrinsic colors of galaxies expected to be observed at faint magnitudes (i.e. at $z > 0$) can now be computed via the assumption of the global properties of the universe, which are specified by the values assigned to the parameters of Friedmann models. This calculation of the past from the present is mediated by the evolutionary models of galaxies. Its results can be expressed in the form $A(m, c)$, which readily allows comparison with observations. Bruzual and Kron's (1980) interpretation of Kron's (1980a) photometry of a complete sample of faint galaxies is an adequate representation of the current state of the art. In Figures 3a and 3b the observed data are compared with model predictions of the $A(m = J)$ and $A(c = J - F)$ distributions, respectively, calculated for the parameters listed in Table 1. For all these $A(m, c)$-models in the Table, a variety of evolutionary galaxy models were selected, whose present age colors match the observed colors of bright galaxies (i.e., at $J \approx 15$). In the case of the no-evolution model, the spectral energy distributions of these representative galaxy models were frozen at $z = 0$, i.e., their colors and magnitudes as a function of redshift were computed from unevolving sources.

The main feature of Figure 3 is the fact that the models are capable of reproducing the observed distributions to first order. This can be taken as to indicate that the general model structure is reasonable in that at least its more important basic building blocks have been identified correctly.

The particular choice of values assigned to the parameters in Table 1 serves to illustrate the sensitivity of the $A(m, c)$-model predictions with respect to the two principal ingredients: the cosmological model and galaxy evolution.

Table 1. Parameters of $A(m, c)$-models.

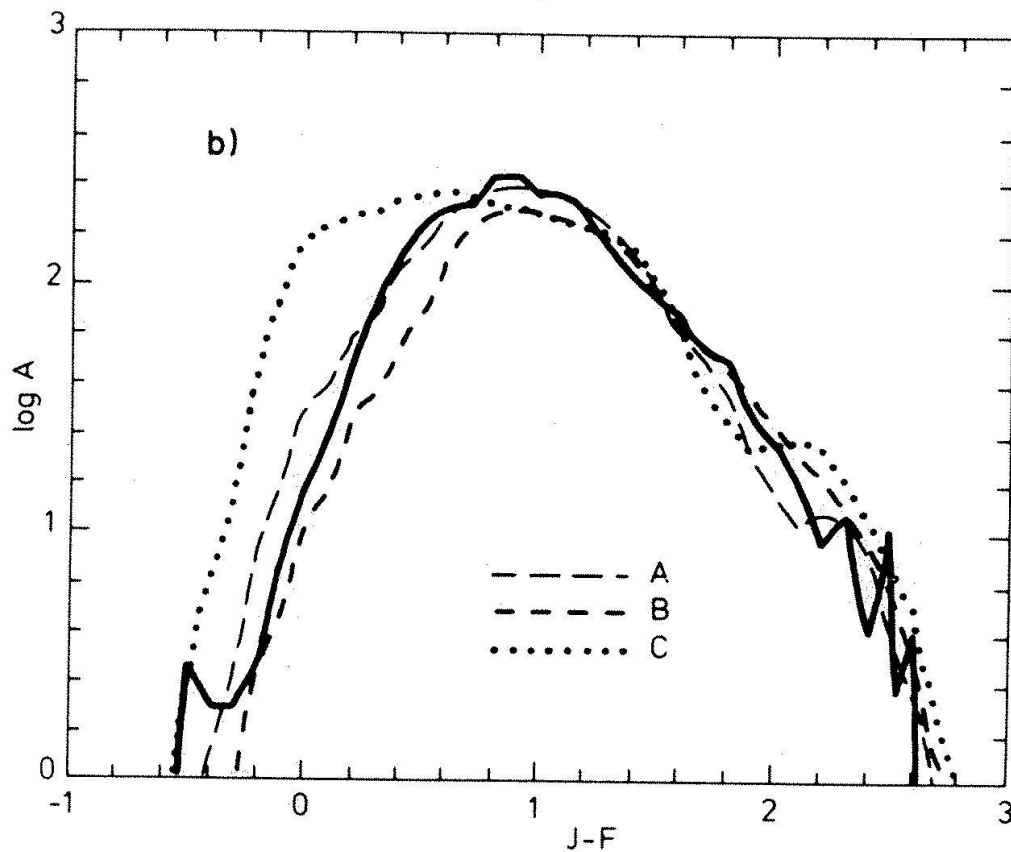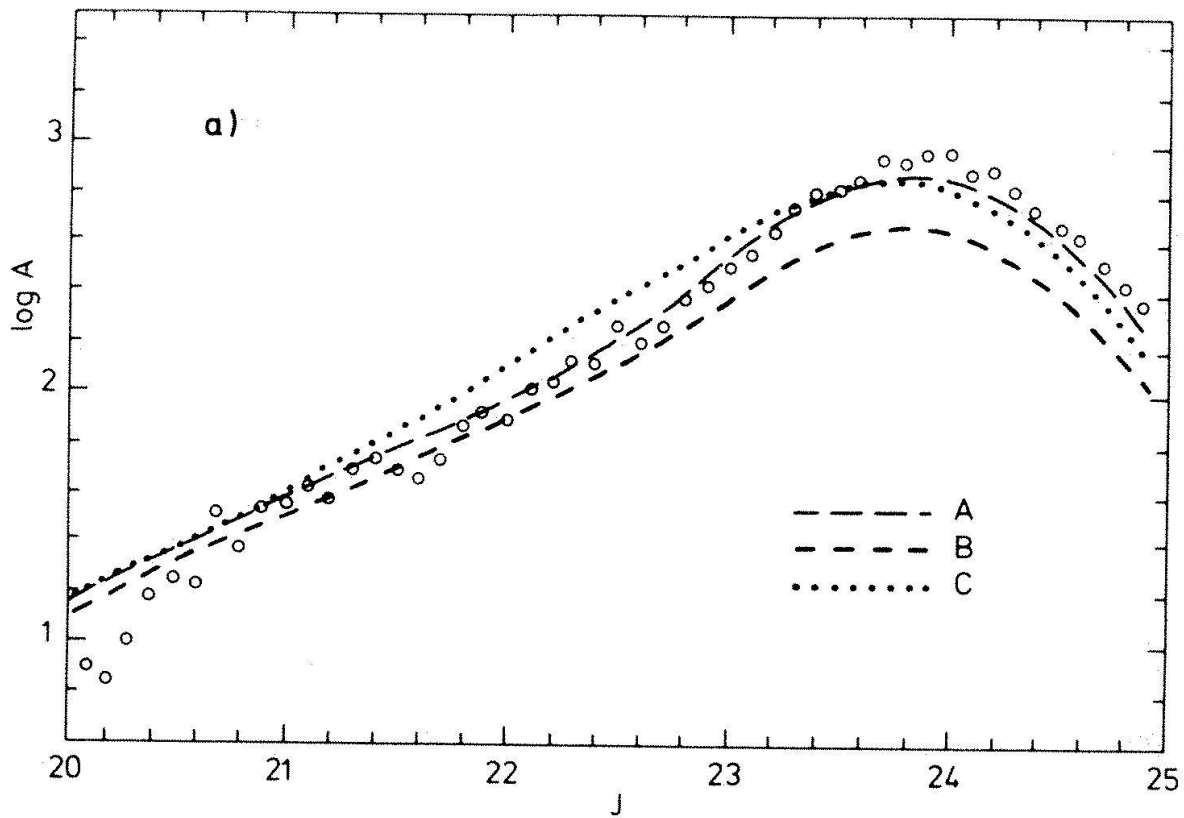| $A(m, c)$-model | Cosmological Model | | Galaxy Models | |
	q_0	H_0 [km s^{-1} Mpc^{-1}]	Present Age, t_0 [Gyr]	Evolution
A	0	60	16	yes
B	0	60	16	no
C	0.5	50	13	yes

Fig. 3. (a) Differential galaxy counts per 0.1 magnitude interval per 1080 square arcmin, as a function of apparent J magnitude. Open circles represent observations by Kron (1980a) in a field centered on Selected Area 57. Curves represent models listed in Table 1, with random errors in J and increasing count incompleteness with increasing J magnitude incorporated.

(b) Differential galaxy counts per 0.1 magnitude interval in J-F color, per 1080 square arcmin, as a function of J-F color, for the magnitude interval $22 \leq (J+F)/2 < 23$. The heavy solid line represents observations by Kron (1980a) in a field centered on Selected Area 57. Other curves represent models listed in Table 1, with random errors in color and magnitude incorporated.

(Figures adapted from Bruzual and Kron 1980.)

The evolutionary effects are demonstrated in Figure 3 by models A and B, whose only difference is that model A has, and model B has not, its galaxy energy distributions evolved. Roughly speaking, the no-evolution model B predicts slightly redder colors (especially on the blue side of the distribution in Figure 3b) and smaller counts (Figure 3a) than observed for $J \gtrsim 22$. The desired improvement, namely to get slightly bluer colors and larger counts at all magnitudes $J \gtrsim 22$, is just about achieved by simply letting the galaxy energy distributions evolve in model A. This behavior is explained by the fact that the evolving galaxy models have higher star formation rates in the past, making them bluer than nonevolving sources at all redshifts (Figure 2a). But then, intrinsically bluer galaxies get dimmer less rapidly with redshift than do redder ones (Figure 2b), so for a given apparent magnitude interval or limit, the bluer galaxies are seen out to larger redshifts (hence distances). The net effect of evolution is then a shift toward bluer average galaxy color and a larger number of galaxies seen at a given (faint) apparent magnitude.

The cosmological effects are demonstrated in Figure 3 by models A and C. While model A ($q_0 = 0$) provides a good fit to the observations in both the number-magnitude and the number-color diagrams, model C ($q_0 = 0.5$) fits both observed distributions poorly, rising too steeply at the brighter magnitudes in Figure 3a, and predicting too many blue galaxies in Figure 3b. These differences in model behavior arise mainly from the different time-redshift and volume-redshift relations involved. At a given redshift, the look-back time is a larger fraction of the adopted present galaxy age, t_0, for $q_0 = 0.5$ than it is for $q_0 = 0$. Therefore, at a given redshift, galaxies are being observed in earlier stages of their evolution in the $q_0 = 0.5$ case than they are in the $q_0 = 0$ case, which means that - in the present picture where galaxies are in general assumed to have had higher star formation rates, i.e. have been evolving more rapidly, at earlier times - these galaxies are also being observed bluer and brighter in a $q_0 = 0.5$ universe. Alternatively, for a given apparent magnitude, the redshifts sampled for $q_0 = 0.5$ span a larger range than for $q_0 = 0$, making the evolutionary effects appear more pronouncedly in

model C than in model A. However, at sufficiently faint apparent magnitudes (or high enough redshifts) in Figure 3a, the number of galaxies predicted from model C drops below the model A results essentially because the size of the volume element at large z is much smaller for $q_0 = 0.5$ than for $q_0 = 0$.

While the models presented in Figure 3 illustrate well their feasibility as possible self-consistent schemes for the interpretation of faint galaxy observations, they do of course not exhaust all possible combinations of parameters. Consequently, even though model A provides a very good fit to the data, no claims of uniqueness can be made. However, the very fact that a successful fit has been found may be summarized in the following conclusion: The universe at faint magnitudes ($J \approx 24$) appears the way it would be expected to appear from extrapolation of what is known about galaxies at bright magnitudes ($J \approx 15$), if a Friedmann cosmological model with $q_0 \approx 0$ is assumed. The case for a $q_0 > 0.5$ universe would require galaxy evolutionary schemes very different from those considered by Bruzual and Kron and by most other authors.

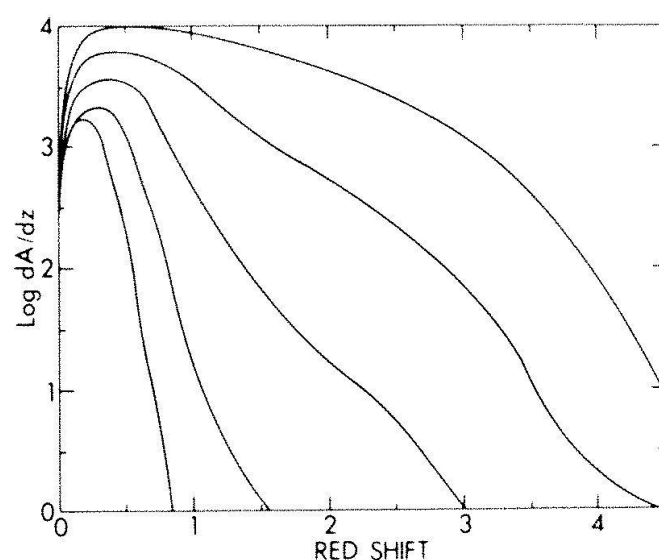The next logical step then consists in finding independent constraints for the histories of

Fig. 4. Distribution of galaxy redshifts as a function of apparent magnitude, predicted for model A in Table 1. Log dA/dz gives the number of galaxies per unit redshift interval. The five curves represent, from top to bottom, intervals of one magnitude centered on $(J + F)/2 = 24.5, 23.5, 22.5, 21.5$, and 20.5. (Figure taken from Bruzual and Kron 1980.)

148

star formation in the different galaxy types. Figure 4 gives, for model A, the distributions of galaxy redshifts predicted at different apparent magnitude levels. The ordinate is the (logarithm of the) number of galaxies per unit redshift interval, and the five curves from top to bottom represent intervals of one magnitude centered on $(J + F)/2 = 24.5$, 23.5, 22.5, 21.5, and 20.5.

What the Figure tells us is that as we go to fainter magnitudes, galaxies of an increasingly large redshift range, and of those an increasingly large fraction of high-redshift galaxies contribute to the counts at each magnitude. According to model A, then, a substantial number of galaxies in Kron's deep survey have been detected at redshifts $z \gtrsim 1.5$. Since the shapes of the redshift distributions of Figure 4 are sensitive to galaxy evolutionary effects, the reality of the assumed underlying histories of the star formation rate can be tested, in principle, by observing the redshifts of a small random subsample of Kron's faint galaxies and examining the corresponding shape(s) of their distribution(s).

This is how we are led back to the determination of redshifts. In order to complete the task as sketched in the first section, one cannot however do with only a few of them. In fact, measuring two or more colors and constructing two-color diagrams for faint galaxies may prove a more practicable solution.

In a two-color diagram, for each galaxy type the theoretical locus of variable redshift is always a well-defined line – as opposed to a scatter diagram –, and the individual loci for different galaxy types are separate. As a result, for the variety of galaxy types there exists in a two-color diagram a similar locus at each redshift, and these individual loci of constant redshift are separate as well, the extent to which they are spread across a two-color plane essentially depending on the choice of the photometric passbands involved in the color measurements.

As an example, Figure 5 shows the two-color diagrams constructed from Kron's (1980b) photographic J,F-system supplemented by an ultraviolet (U) and a near-infrared (N) passband. Constant-redshift loci were computed from Bruzual's (1981) evolutionary galaxy models described above. Note that
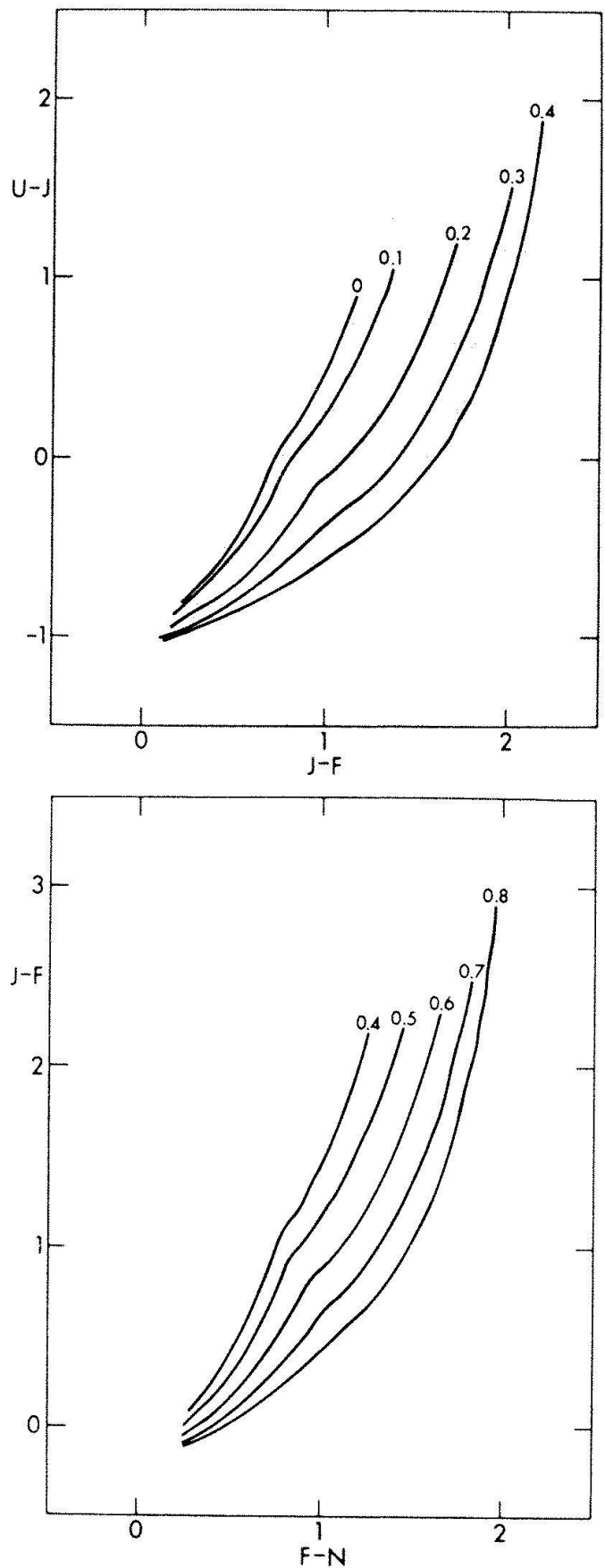

Fig. 5. Two-color diagrams for Kron's UJFN photographic broad-band system. Curves are loci of constant redshift, as labeled, computed for evolving galaxy models with present-day colors matching the range observed for bright galaxies.
(Figure taken from Kron 1980b.)

the two diagrams display useful sensitivities to different redshift ranges; this is due mainly to the existence in galaxy spectra of a break in continuum slope around 4000 Å, which is shifted into the redder passbands at higher values of z (see Figure 1).

In principle, then, the general properties of two-color diagrams offer a powerful tool for fast determination of types and redshifts for large numbers of galaxies. It is now largely left to the practice of multicolor photometry to keep this promise of the principle.

Acknowledgements

References

Bruzual, A.G., 1981, Ph.D. thesis, University of California, Berkeley.
—   , Kron, R.G. 1980, Astrophys. J. 241, 25.
Kron, R.G., 1980a, Astrophys. J. Suppl. 43, 305.
—   1980b, in: Two Dimensional Photometry, P. Crane, K. Kjär (eds), ESO Workshop Proceedings, Noordwijkerhout, p.349.
Salpeter, E.E., 1955, Astrophys. J. 121, 161.
Sandage, A.R., 1961, Astrophys. J. 134, 916.
Tinsley, B.M., 1980, Astrophys. J. 241, 41.

Address of the author:

PD Dr. Roland Buser
Astronomical Institute
University of Basle
CH-4102 Binningen BL (Switzerland)